Electronic Supplementary Material (ESI) for CrystEngComm.

Supporting Information

Epoxide activation by a silver phosphonate for heterogeneous catalysis of CO_2 cycloaddition

Chao-Ying Gao,[⊥*ab] Chen Mao,[⊥ab] Yang Yang,[a] Ning Xu,[a] Jinglin Liu,[a] Xiaohong Chen,[a] Jinghai Liu,[*ab] and Limei Duan[*ab]

a. College of Chemistry and Materials Science, Inner Mongolia Minzu University (IMMN), Tongliao 028043, Inner Mongolia, People's Republic of China. Email:chaoyinggao@163.com; jhliu2008@sinano.ac.cn.; duanlmxie@126.com;

b. Inner Mongolia Key Lab of Carbon Nanomaterials, Nano Innovation Institute (NII), Inner Mongolia Minzu University (IMMN), Tongliao 028000, People's Republic of China

⊥ *These authors contributed equally.*

Supplementary Index

Contents

S1. Materials and Methods

1.1 General information

Materials and Instrument

All commercial chemicals were used without further purification except for organo-phosphonate ligand H_8L, which was synthesized by a modified procedure documented previously.[1]

Powder X-ray diffraction (PXRD) was carried out with a MiniFlex 600 X-ray powder diffractometer equipped with a Cu sealed tube (λ = 1.541 78 Å) at 40 kV and 40 mA. Elemental analyses for C, H, and N were performed by a VarioEL analyzer. Thermal gravimetric analysis (TGA) was conducted under an air atmosphere with a heating rate of 10 ^{o}C/min on a SDT 2960 Simultaneous DSC-TGA of TA instruments up to 800 ^{o}C. The infrared (IR) spectra (diamond) were recorded on a Nicolet 7600 FT-IR spectrometer within the 4000-500 cm^{-1} region. ^{1}H NMR spectra were carried out in $CDCl_3$ solvent on a Bruker 400 MHz spectrometer. The chemical shift is given in dimensionless δ values and is referenced relative to TMS in ^{1}H spectroscopy. Yields were determined by GC analysis using methanol as the solvent. (Shimadzu GC-2014 equipped with a capillary column (HP-5, 30 m × 0.25 μm × 0.32 mm) using a flame ionization detector. Heating method: 50 °C for 2 min and then warming up to 300 °C (heating rate: 15 °C/min). Scanning electron microscopy (SEM, Hitachi S-4800) coupled with an energy dispersive X-ray spectroscopy (EDS) was used to determine the morphologies and element analysis of the samples.

1.2 Single-Crystal X-ray Crystallography

Single-crystal X-ray diffraction (SXRD) data of compound $[Ag_{10}(H_3L)_2(H_2O)2(4,4'\text{-bipy})$ were collected on a Bruker diffractometer using Mo *Ka* radiation (λ = 1.54178 Å) at 293 K. Data processing was accomplished with the SAINT processing program.[2] The structure was solved by the direct methods and refined by full-matrix least-squares fitting on F^2 using the SHELXTL crystallographic software package.[3] Non-hydrogen atoms were refined with anisotropic displacement parameters during the final cycles. All hydrogen atoms of the organic molecule were placed by geometrical considerations and were added to the structure factor calculation. The final formula of $[Ag_{10}(H_3L)_2(H_2O)_2(4,4'\text{-bipy})$ was determined mainly determined by single-crystal X-ray diffraction, combining charge equilibrium consideration, thermogravimetric analysis (TGA) and elemental analysis.

Elemental analysis: Calculated for $Ag_{10}P_8C_{62}N_2O_{26}H_{50}$ (MW 2565.53): C, 29.03; N, 1.09; H, 1.96. Found: C, 29.15; N, 1.06; H, 1.98.

Crystallographic data for $Ag_{10}P_8C_{62}N_2O_{26}H_{50}$ (CCDC: 2203855) has been deposited with Cambridge Crystallographic Data Centre. Data can be obtained free of charge upon request at www.ccdc.cam.ac.uk/data_request/cif. Crystal data and structure refinement is summarized in Table S1.

1.3 Cycloaddition of CO_2 to epoxides

Yields except for the final ones were calculated by GC using n-dodecane as internal standard substance, and the final products and corresponding conversions were determined and by ^{1}H NMR spectroscopy.

The conversion was calculated from ^{1}H NMR according to the following equation.

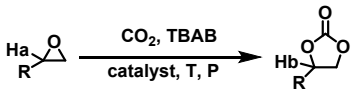

$$\text{conversion} = \frac{^1\text{Hb}}{(^1\text{Ha} + ^1\text{Hb})}$$

S2 Supplementary tables and figures

Table S 1 Crystallographic data

Formula	$Ag_{10}P_8C_{62}N_2O_{26}H_{50}$
F_w	2565.53
Temperature, K	293(2)
Crystal system	Triclinic
Radiation source	Mo $K\alpha$
Space group	*P-1*
a, Å	10.7786(6)
b, Å	12.6891(7)
c, Å	14.2722(8)
α, deg	77.4970(10)
β, deg	86.2210(10)
γ, deg	67.3010(10)
V, Å^3	7875.5(10)
Z	2
D_c, mg/mm^3	2.420
μ, mm^{-1}	2.987
F (000)	1230
reflection collected	10528
Total/unique reflections	10528 / 6915
R_{int}	0.0637
GOF on F^2	0.983
R_1/wR_2 (I > 2σ(I))	0.0307/ 0.0986
R_1/wR_2 (all data)	0.0366 / 0.1286
Largest diff. peak/hole / (e Å^{-3})	1.148 and /-1.485

$R_1=\sum||F_o|-|F_c||/\sum|F_o|$. $wR_2=[\sum[w\,(F_o^2-F_c^2)^2]\,/\,\sum[\,w\,(F_o^2)^2]]^{1/2}$

Table S2. Selected bond lengths [Å] and angles [°]for **1**

Ag(1)-O(12)#1	2.250(4)	Ag(3)-N(1)	2.221(5)
Ag(1)-O(2)#2	2.283(4)	Ag(3)-O(2)#4	2.333(4)
Ag(1)-O(8)	2.485(4)	Ag(3)-O(8)#5	2.438(4)
Ag(1)-O(8)#3	2.553(4)	Ag(3)-O(12)	2.549(4)
Ag(1)-Ag(1)#3	2.9584(9)	Ag(4)-O(14)	2.326(5)
Ag(2)-O(11)	2.227(4)	Ag(4)-O(5)#6	2.360(4)
Ag(2)-O(9)#1	2.244(4)	Ag(4)-O(7)#5	2.361(4)
Ag(2)-O(6)#2	2.597(5)	Ag(4)-O(12)	2.432(4)
Ag(5)-O(7)#5	2.234(4)	Ag(5)-O(3)#8	2.341(4)
Ag(5)-O(9)#7	2.244(4)	Ag(5)-O(6)#6	2.559(4)
O(3)-Ag(5)#8	2.341(4)	O(5)-Ag(4)#6	2.360(4)
O(6)-Ag(5)#6	2.559(4)	O(6)-Ag(2)#2	2.597(5)
O(7)-Ag(5)#10	2.234(4)	O(7)-Ag(4)#10	2.361(4)
O(8)-Ag(3)#10	2.438(4)	O(8)-Ag(1)#3	2.553(4)
O(9)-Ag(5)#7	2.244(4)	O(9)-Ag(2)#1	2.244(4)
O(12)-Ag(1)#1	2.250(4)		
O(12)#1-Ag(1)-O(2)#2	164.74(15)	O(12)#1-Ag(1)-O(8)	114.84(14)
O(2)#2-Ag(1)-O(8)	78.94(14)	O(12)#1-Ag(1)-O(8)#3	84.62(14)
O(2)#2-Ag(1)-O(8)#3	97.60(14)	O(8)-Ag(1)-O(8)#3	108.10(10)
O(12)#1-Ag(1)-Ag(1)#3	105.78(11)	O(2)#2-Ag(1)-Ag(1)#3	87.31(11)
O(8)-Ag(1)-Ag(1)#3	55.11(9)	O(8)#3-Ag(1)-Ag(1)#3	52.99(9)
O(11)-Ag(2)-O(9)#1	132.73(15)	O(11)-Ag(2)-O(6)#2	136.97(14)
O(9)#1-Ag(2)-O(6)#2	83.51(14)	N(1)-Ag(3)-O(2)#4	143.13(17)
N(1)-Ag(3)-O(8)#5	119.29(16)	O(2)#4-Ag(3)-O(8)#5	78.99(14)
N(1)-Ag(3)-O(12)	122.02(16)	O(2)#4-Ag(3)-O(12)	90.79(13)
O(8)#5-Ag(3)-O(12)	81.04(13)	O(14)-Ag(4)-O(5)#6	98.99(16)
O(14)-Ag(4)-O(7)#5	117.19(16)	O(5)#6-Ag(4)-O(7)#5	116.56(14)
O(14)-Ag(4)-O(12)	121.36(16)	O(5)#6-Ag(4)-O(12)	117.42(14)
O(7)#5-Ag(4)-O(12)	86.80(13)	O(14)-Ag(4)-Ag(5)	83.67(13)
O(5)#6-Ag(4)-Ag(5)	91.49(10)	O(7)#5-Ag(4)-Ag(5)	48.10(10)
O(12)-Ag(4)-Ag(5)	134.66(9)	O(7)#5-Ag(5)-O(9)#7	142.65(15)
O(7)#5-Ag(5)-O(3)#8	114.35(15)	O(9)#7-Ag(5)-O(3)#8	102.07(15)

O(7)#5-Ag(5)-O(6)#6	104.11(15)	O(9)#7-Ag(5)-O(6)#6	84.41(15)
O(3)#8-Ag(5)-O(6)#6	88.03(14)	O(7)#5-Ag(5)-Ag(4)	51.86(10)
O(9)#7-Ag(5)-Ag(4)	96.00(11)	O(3)#8-Ag(5)-Ag(4)	156.64(12)
O(6)#6-Ag(5)-Ag(4)	79.07(10)	O(7)#5-Ag(5)-Ag(5)#9	85.02(11)
O(9)#7-Ag(5)-Ag(5)#9	74.47(10)	O(3)#8-Ag(5)-Ag(5)#9	110.38(11)

Symmetry transformations used to generate equivalent atoms: #1: -x+1, -y, -z+1; #2: -x+1, -y, -z; #3: -x+1, -y-1, -z+1; #4 -x+1, -y+1, -z; #5 x, y+1, z; #6 -x+2, -y, -z; #7: -x+2, -y, -z+1; #8: -x+2, -y+1, -z; #9: -x+2, -y+1, -z+1; #10 x, y-1, z.

Table S3 Comparison with different MOF catalysts in the cycloaddition reaction of CO_2 and epichlorohydrin.

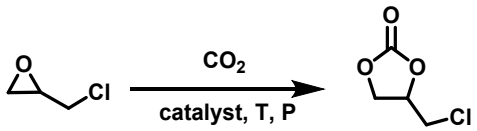

Catalyst	Co-cat.	Cat. / co-cat. (mmol)	T (K)	P (MPa)	T (h)	Yield (%)	TON	TOF (h^{-1})	Ref.
Gea-MOF-1	*n*-Bu_4NBr	0.15 / 0.15	393	2.0	6	89	593	99	4
CHB (M)	*n*-Bu_4NBr	1.6 / 1.6	393	1.2	6	72	44.6	7	5
Ni(salphen)-MOF	*n*-Bu_4NBr	2.8 / 3.0	353	2.0	4	84	300	75	6
ZnMOF-1-NH_2	*n*-Bu_4NBr	1.0 / 2.5	353	0.8	8	89	84.8	10.6	7
NUC-30	*n*-Bu_4NBr	1.0 / 5.0	333	1.0	12	96	96	8	8
1	*n*-Bu_4NBr	0.01 / 0.3	373	1.0	6	87	8700	1450.0	This work

Table S4. Comparison with different MOF catalysts reported in the cycloaddition reaction of CO_2 and styrene oxide.

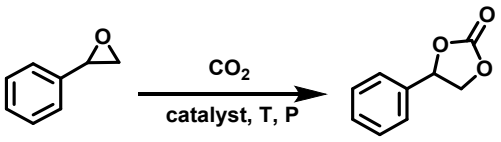

Catalyst.	Co-Catalyst	Cat./Co-cat. (mmol)	T (K)	P (MPa)	T(h)	Yield (%)	TON	TOF (h^{-1})	Ref.
NUC-30	*n*-Bu_4NBr	1.0 / 5.0	333	1.0	12	92	92	7.67	8
NH_2-MIL-101(Al)	*n*-Bu_4NBr	0.17 / 0.14	393	1.8	6	96	564.7	94.1	9
Ni-TCPE-1	*n*-Bu_4NBr	0.5 / 1.5	373	1.0	12	99	2000	167	10
Ni-TCPE-2	*n*-Bu_4NBr	0.5 / 1.5	373	1.0	12	86.2	1720	143	10
Gea-MOF-1	*n*-Bu_4NBr	0.15/ 0.15	393	2.0	6	85	567	94.5	4
Ni(salphen)-MOF	*n*-Bu_4NBr	2.8 / 3.0	353	2.0	4	81	289	72	6
CHB(M)	*n*-Bu_4NBr	1.6 /1.6	393	1.2	6	56	35	6	5
1	*n*-Bu_4NBr	0.05 / 1.5	373	1.0	12	68.5	1370	114.2	This work

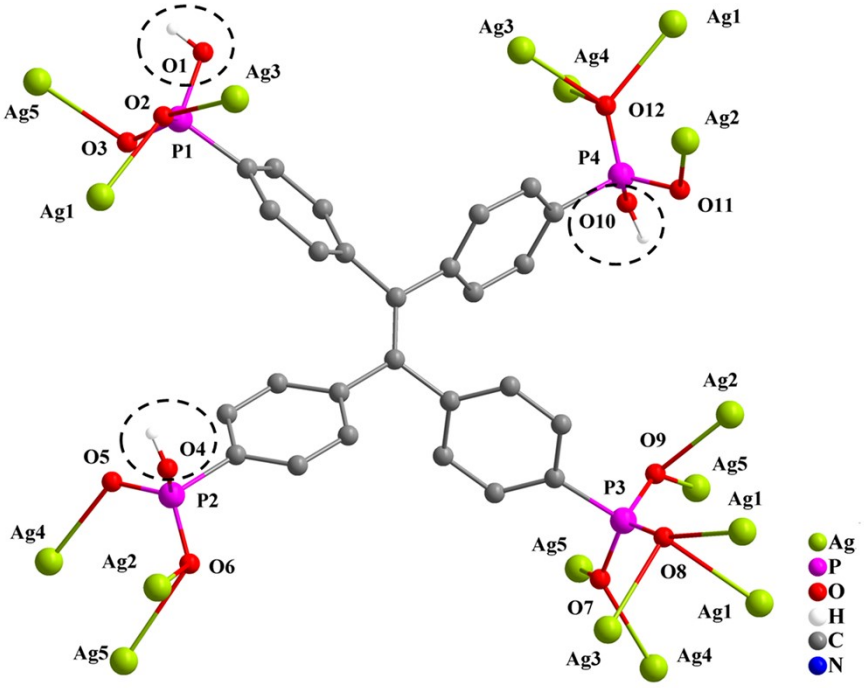

Figure S1. The representation of the deprotonated mode for H_3L^{5-}.

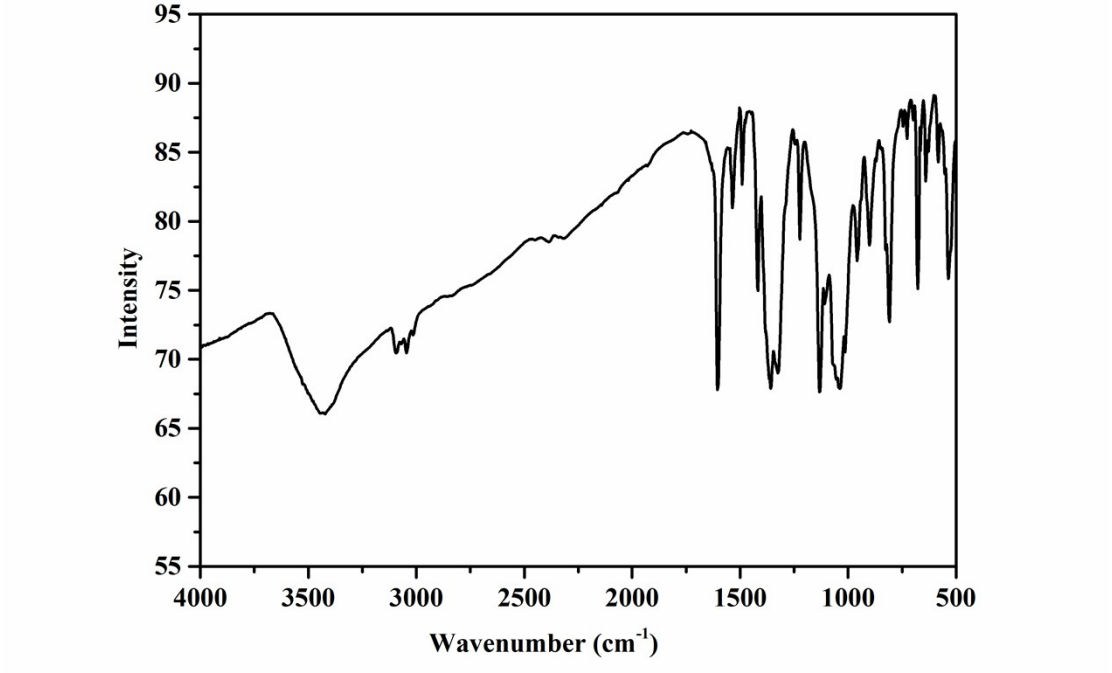

Figure S2. Infrared spectra of the compound **1**.

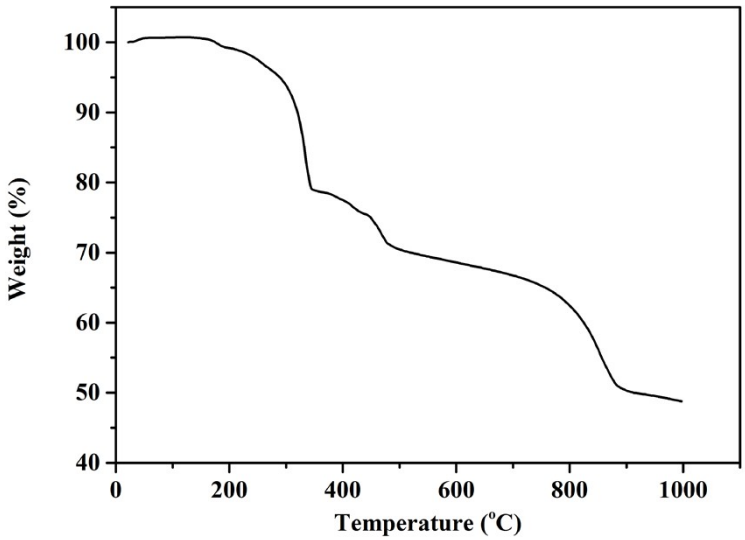

Figure S3. TG curve of compound **1**.

The thermal stabilities of the silver phosphate were studied using thermogravimetric analysis (TGA) under N_2 atmosphere. The TGA curve indicates that water molecules coordinated to Ag(I) centers were lost from room temperature (RT) to 230 °C with a weight loss of 1.61% (calcd: 1.40%). Then the TGA curve undergo continue weightlessness with decomposition of the phosphate and 4,4'-biby ligands, in other word, compound **1** starts to fall into decomposition after about 230 °C.

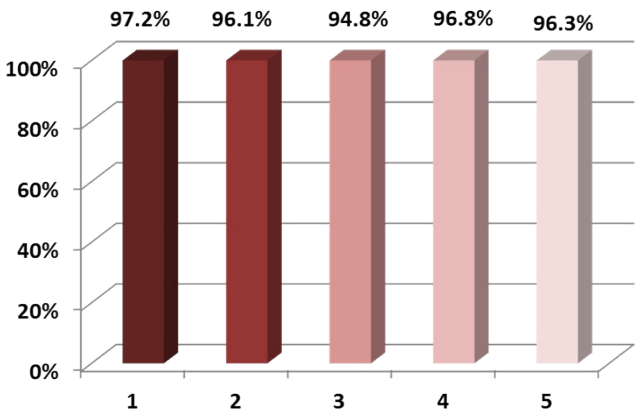

Figure S4. Histogram of recyclibility study (five cycles) for catalytic acitivities of catalyst **1** in coupling of epichlorohydrin with CO_2.
Reaction condition: 60 mmol of epichlorohydrin, 0.01 mmol of catalyst, P = MPa, T = 100 °C, t = 6 h.

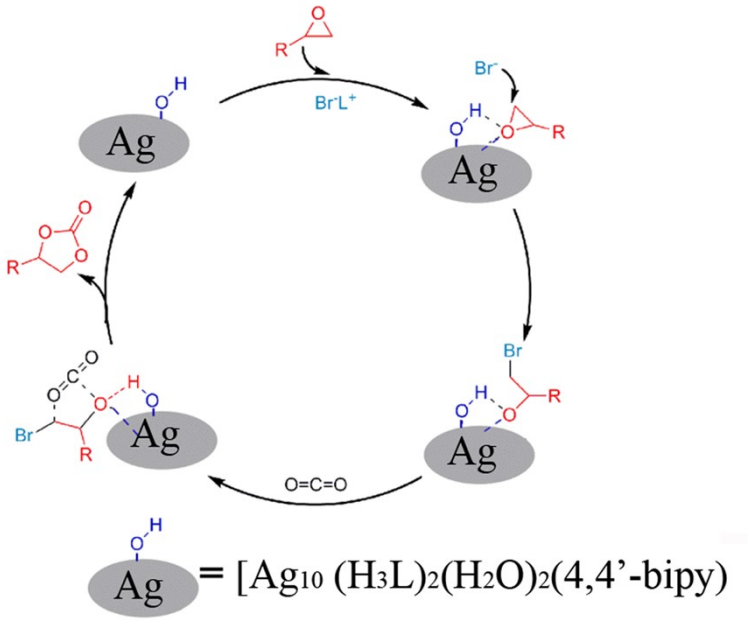

Scheme S1 The proposed mechanism for the cycloaddition of CO_2 and epoxide at the solid/liquid interface assisted by bifunctional catalysis from Lewis acid and Brønsted acid (**L^+** = tetra-n-butylammonium).

S3. The NMR spectrums

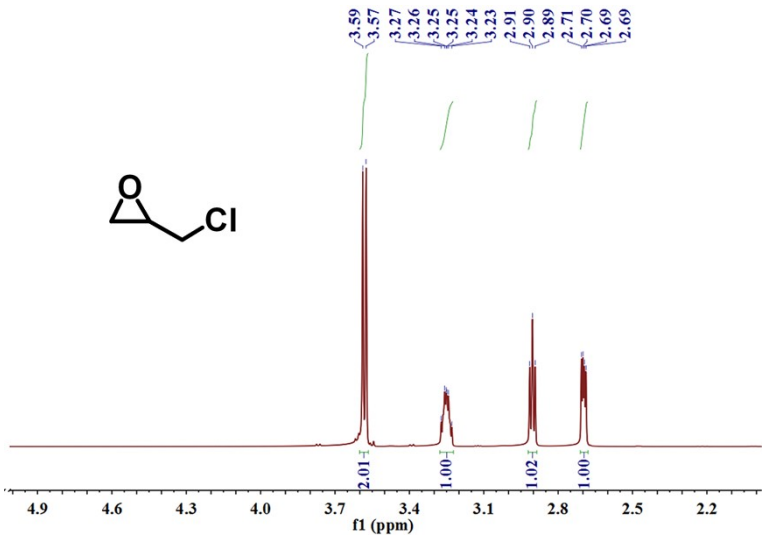

Figure S5 ^{1}H NMR spectra of epichlorohydrin (400 MHz, $CDCl_3$): δ = 3.57-3.59 (d, J = 8.0 Hz, 2H,Cl-CH_2), 3.23 – 3.27 (m, 1H,O-CH), 2.89-2.91 (t, J = 4.0 Hz, 1H,O-CH_2), 2.69-2.71 (q, J = 4.0 Hz, 1H, O-CH_2.

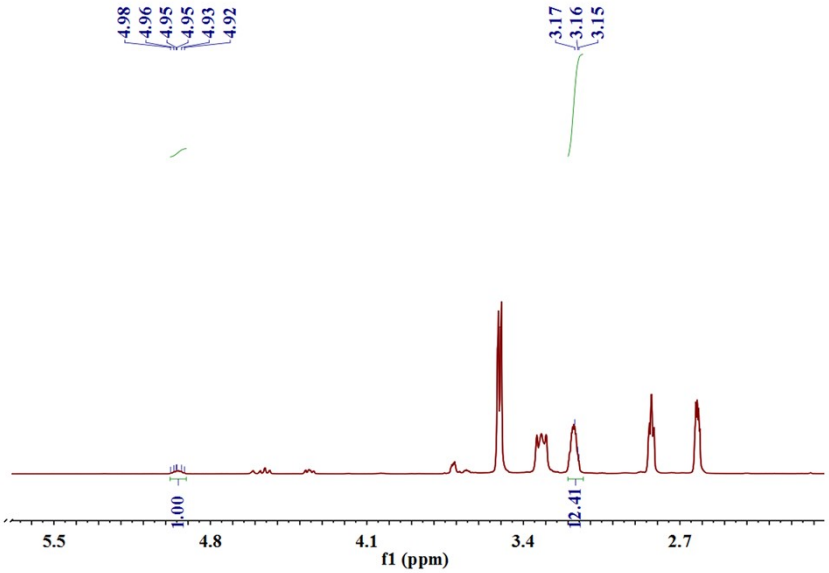

Figure S6 ^{1}H NMR spectra of the cycloaddition product of epichlorohydrin and CO_2 (400 MHz, $CDCl_3$) : δ = 4.92-4.98 (m, 1H, COO-CH), 3.15-3.17 (m, 1H, O-CH_2).
Reaction conditions: epoxide (20 mmol), catalyst (0.01 mmol) and TBAB (0.3 mmol),
T = 25 ^{o}C, P = 1 Pa, t = 12 h; Conversion = 7.5%.

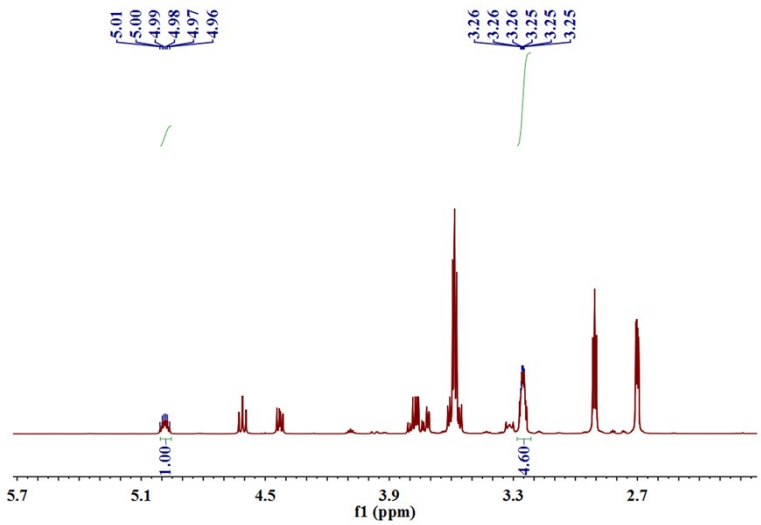

Figure S7 ^{1}H NMR spectra of the cycloaddition product of epichlorohydrin and CO_2 (400 MHz, $CDCl_3$) : δ = 4.96-5.01 (m, 1H, COO-CH), 3.25– 3.26 (m, 1H, O-CH_2).
Reaction conditions: epoxide (20 mmol), catalyst (0.01 mmol) and TBAB (0.3 mmol),
T = 25 °C, P = 1 MPa, t = 12 h; Conversion = 17.8%.

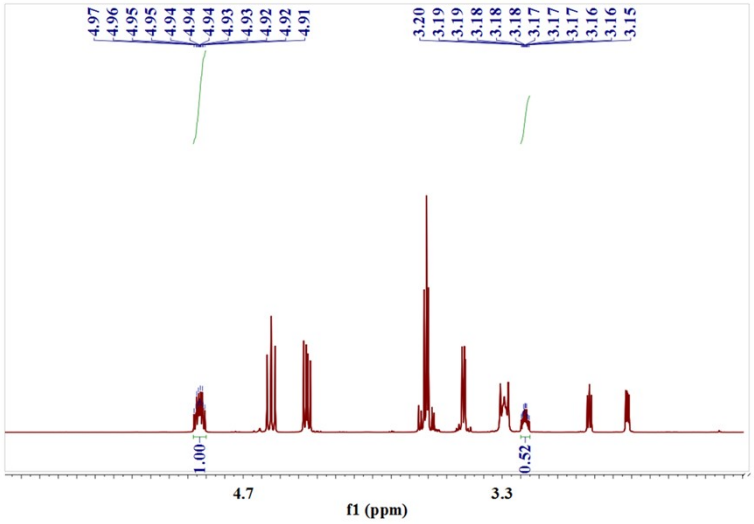

Figure S8 ^{1}H NMR spectra of the cycloaddition product of epichlorohydrin and CO_2 (400 MHz, $CDCl_3$) : δ = 4.91-4.97 (m, 1H, COO-CH), 3.15 – 3.20 (m, 1H, O-CH_2).
Reaction conditions: epoxide (20 mmol), catalyst (0.01 mmol) and TBAB (0.3 mmol), T = 60 °C, P = 1 MPa, t = 12 h; Conversion = 65.8%.

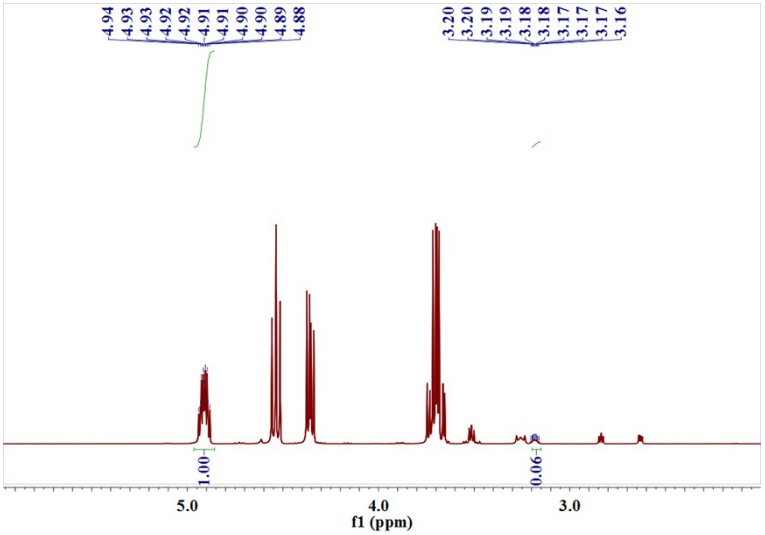

Figure S9 ^{1}H NMR spectra of the cycloaddition product of epichlorohydrin and CO_2 (400 MHz, $CDCl_3$) : δ = 4.88 -4.94 (m, 1H, COO-CH), 3.16 -3.20 (m, 1H, O-CH_2).

Reaction conditions: epoxide (20 mmol), catalyst (0.01 mmol) and TBAB (0.3 mmol), T = 80 °C, P = 1 MPa, t = 12 h; Conversion = 94.3%.

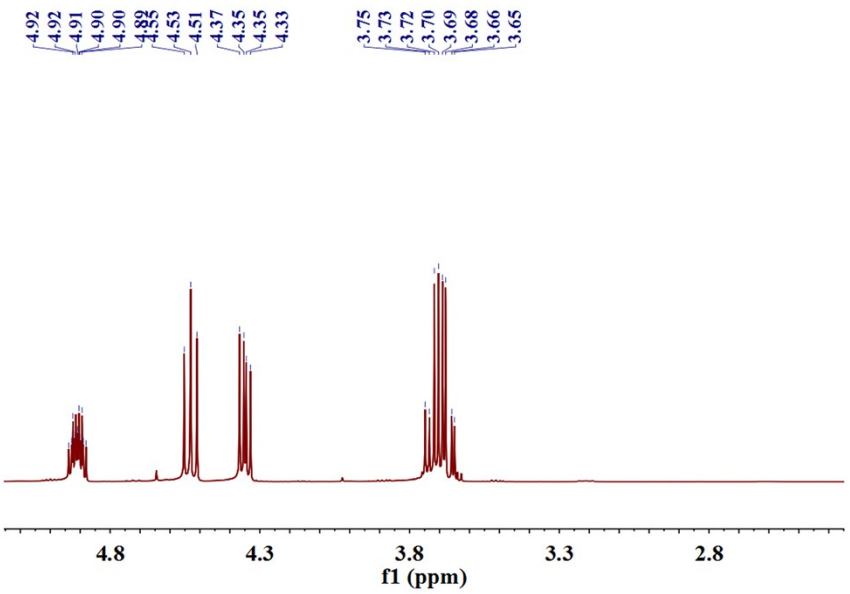

Figure S10 ^{1}H NMR spectra of the cycloaddition product of epichlorohydrin and CO_2 (400 MHz, $CDCl_3$)

Reaction condition: epoxide (20 mmol), catalyst (0.01 mmol) and TBAB (0.3 mmol), T = 100 °C, P = 1 MPa, t = 6 h. Conversion: ＞ 99%

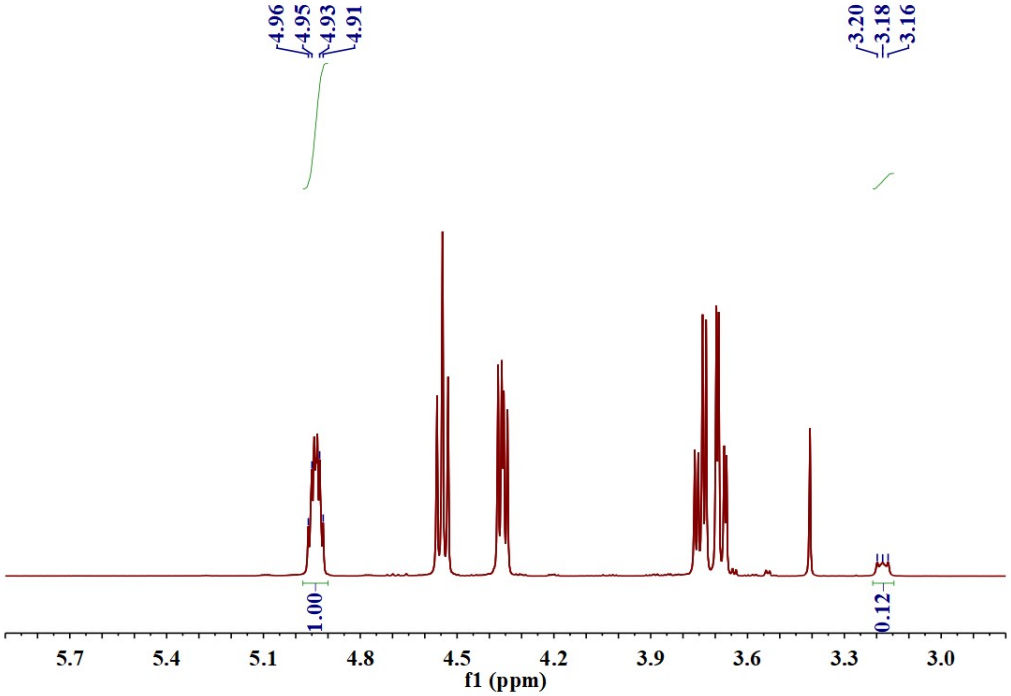

Figure S11 ^{1}H NMR spectra of the cycloaddition product of epichlorohydrin and CO_2 (400 MHz, $CDCl_3$). δ: 4.91 -4.96 (m, 1H, COO-CH), 3.16 -3.20 (m, 1H, O-CH_2).
Reaction condition: epoxide (20 mmol), $AgNO_3$ (0.01 mmol) and TBAB (0.3 mmol), T = 100 °C, P = 1 MPa, t = 3 h. Conversion = 89.3%

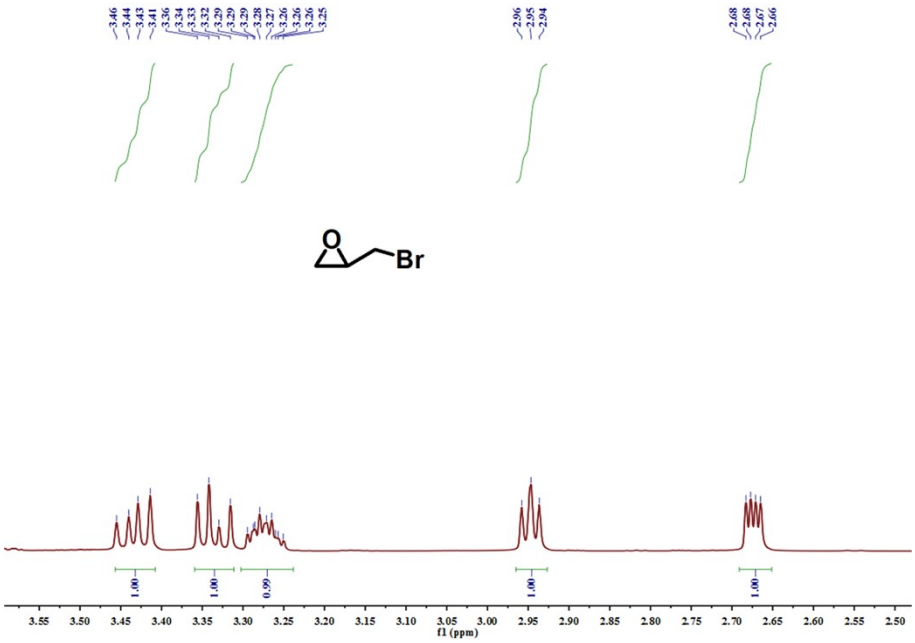

Figure S12 ^{1}H NMR spectra of epibromohydrin (400 MHz, $CDCl_3$): δ = 3.41-3.46 (q, J = 8.0 Hz, 1H, Br-CH_2), 3.33 (q, J = 8.0 Hz, 1H, Br-CH_2), 3.25 – 3.28(m, 1H, O-CH*), 2.94-2.96 (t, J = 4.0 Hz, 1H, O-CH_2), 2.66-2.68 (q, J = 4.0 Hz, 1H, O-CH_2).

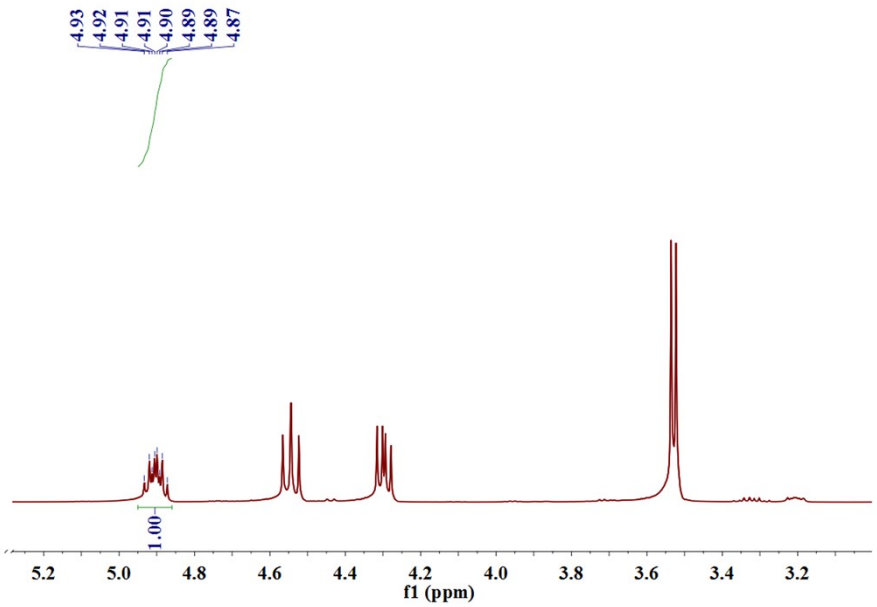

Figure S13. ^{1}H NMR spectra of the cycloaddition product of epibromohydrin and CO_2 for 6h (400 MHz, $CDCl_3$): δ = 4.87-4.93 (m, 1H, COO-CH* of product).

Reaction condition: epoxide (20 mmol), catalyst (0.01 mmol) and TBAB (0.3 mmol), T = 100 °C, P = 1 MPa, t = 6 h. Conversion: ＞ 99%

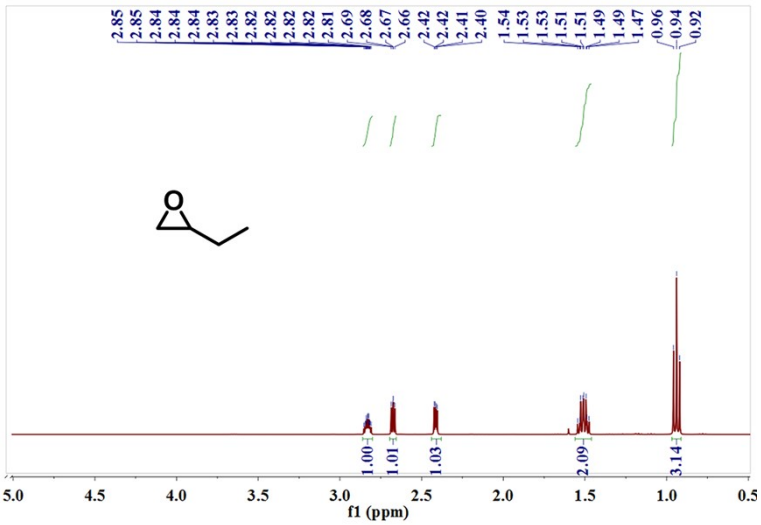

Figure S14. ^{1}H NMR spectra of epoxybutane (400 MHz, $CDCl_3$): δ = 2.81-2.85 (m, 1H, O-CH*), 2.67 (t, J = 5.0, 4.0 Hz, 1H, O-CH_2), 2.40-2.42 (m, 1H, O-CH_2), 1.47-1.54 (m, 2H, -CH_2), 0.92-0.96 (t, J = 7.5 Hz, 3H, -CH_3).

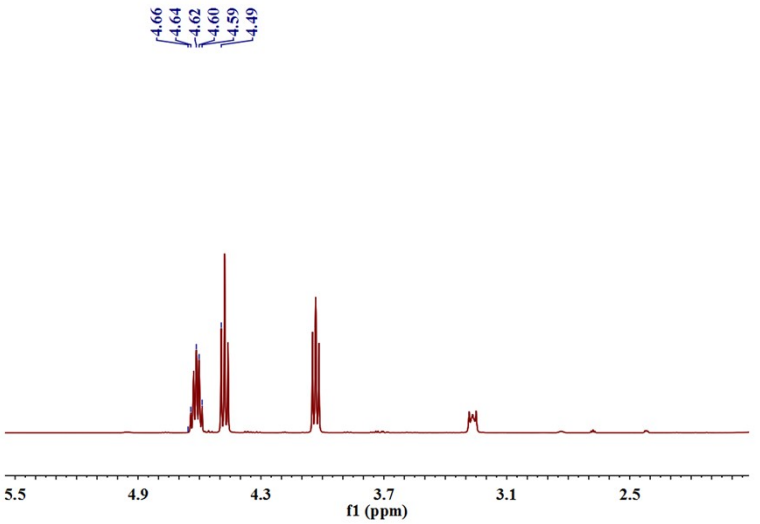

Figure S15. ^{1}H NMR spectra of the cycloaddition product of epoxybutane and CO_2 (400 MHz, $CDCl_3$) : δ = 4.49 – 4.66 (m, 1H, COO-CH* of product).

Reaction condition: epoxide (20 mmol), catalyst (0.01 mmol) and TBAB (0.3 mmol), T = 100 ^{o}C, P = 1 MPa, t = 12 h. Conversion: ＞ 99%

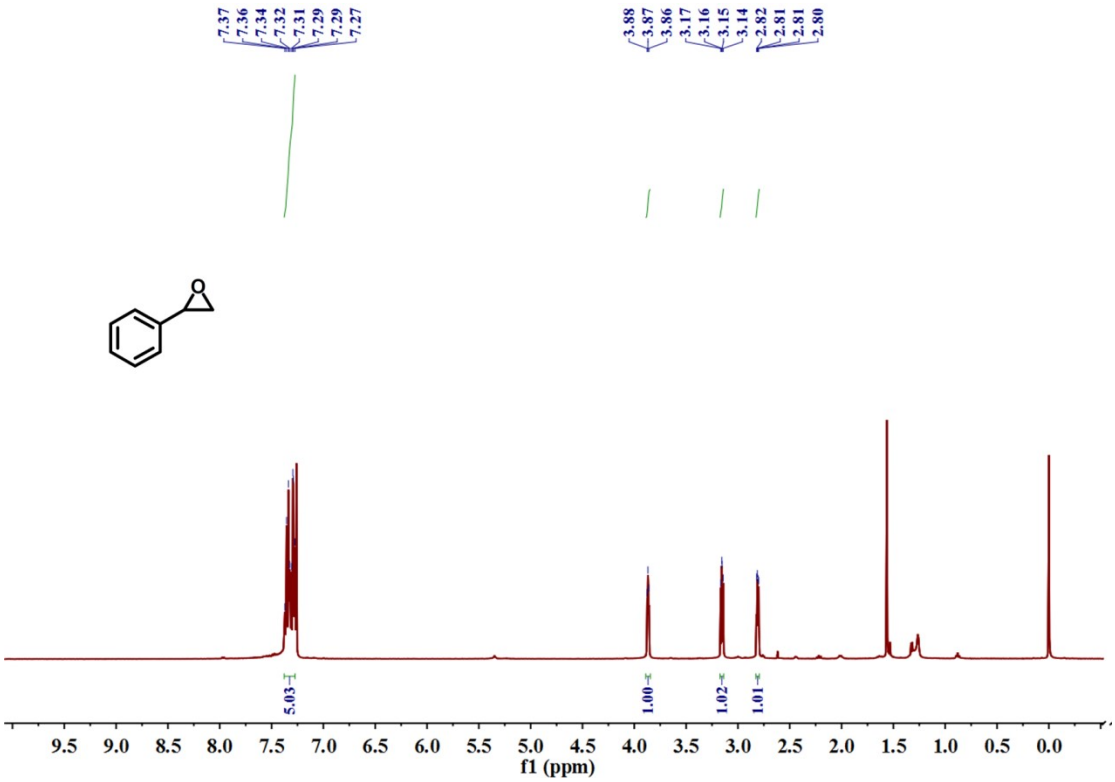

Figure S16. ^{1}H NMR spectra of styrene oxide (400 MHz, $CDCl_3$): δ = 7.27 – 7.37 (m, 5H, Ar-H), 3.86-3.88 (t, J=4.0 Hz, 1H, O-CH), 3.14-3.17 (q, J=4.0 Hz, 1H, O-CH_2), 2.80-2.82 (q, J = 4.0 Hz, 1H, O-CH_2).

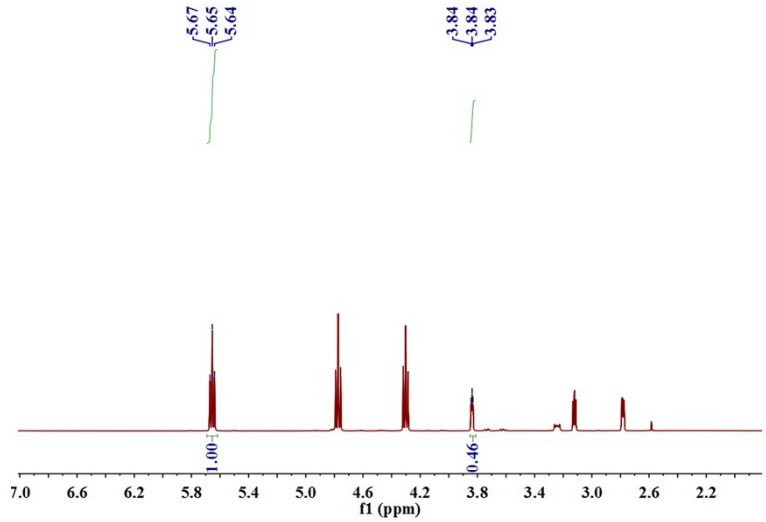

Figure S17. ^{1}H NMR spectra of the cycloaddition product of styrene oxide and CO_2 for 12h (400 MHz, $CDCl_3$) : δ = 5.64-5.67 (t, J = 8.0 Hz, 1H, COO-CH* of product), 3.83-3.84 (t, J = 8.0 Hz, 2.20H, O-CH* of raw material).

Reaction condition: epoxide (20 mmol), catalyst (0.01 mmol) and TBAB (0.3 mmol), T = 100 ^{o}C, P = 1 MPa, t = 12 h; Conversion = 68.5%.

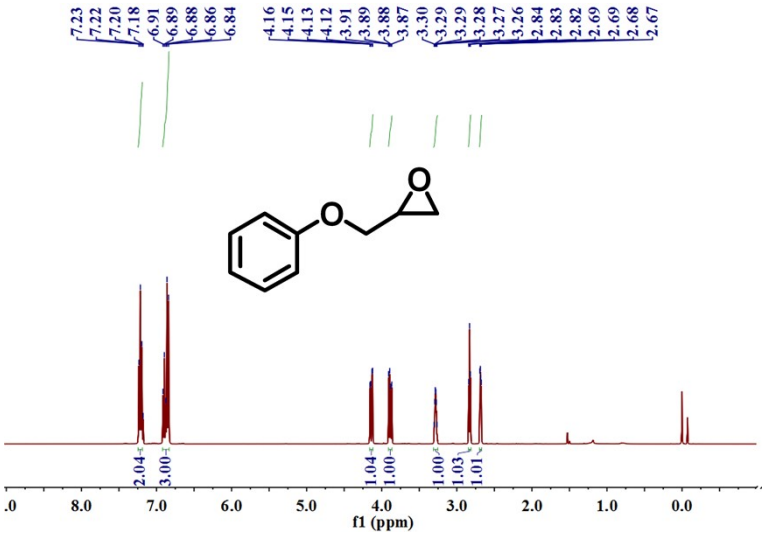

Figure S18. ^{1}H NMR spectra of 1,2-epoxy-3-phenoxypropane (400 MHz, $CDCl_3$) : δ = 7.18-7.23 (m, 2H, Ar-H), 6.84-6.91 (m, 3H, Ar-H), 4.14 (q, J = 4.0 Hz, 1H, ArO-CH_2), 3.88 (q, J = 4.0 Hz, 1H, ArO-CH_2), 3.26-3.30 (m, 1H,O-CH*), 2.83 (t, J = 4.0 Hz, 1H,O-CH_2), 2.68 (q, J = 4.00 Hz, 1H,O-CH_2).

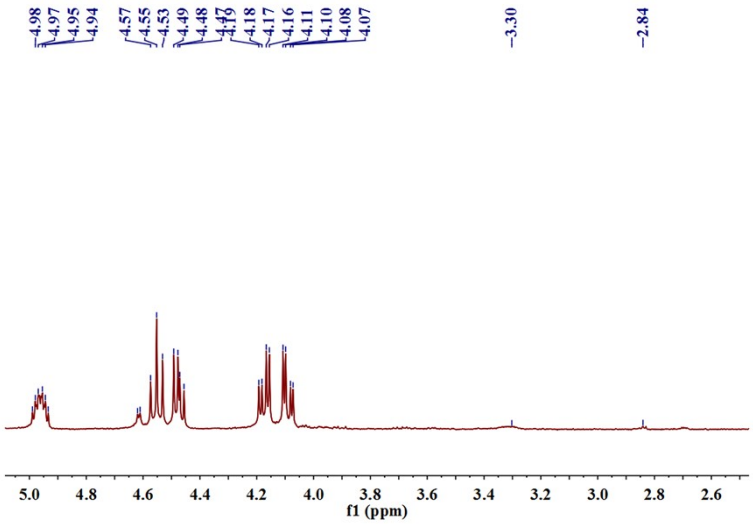

Figure S19. ^{1}H NMR of the cycloaddition product of 1,2-epoxy-3-phenoxypropane and CO_2 (400 MHz, $CDCl_3$): 4.94 - 4.98 (m, 1H, COO-CH), 4.55 (t, J = 8.0 Hz, 1H, COO-CH_2), 4.47 (t, J = 8.0 Hz, 1H, COO-CH_2), 4.19-4.16 (m, 1.46H, 1H -ArO-CH_2 of product and 0.46H -ArO-CH_2 of 1,2-epoxy-3-phenoxypropane), 4.07-4.11 (dd, J = 8.0 Hz, 4.0 Hz, 1H, ArO-CH_2 of product), 3.30 (q, J = 8.0 Hz, 0.46H, ArO-CH2 of 1,2-epoxy-3-phenoxypropane), 2.84 (t, J = 4.0 Hz, 0.46H, O-CH_2).
Reaction condition: epoxide (20 mmol), catalyst (0.01 mmol) and TBAB (0.3 mmol), T = 100 ^{o}C, P = 1 MPa, t = 12 h; Conversion ＞ 99%.

S4 References

1. D. Chakraborty, D. Musib, R. Saha, A. Das, M. K. Raza, V. Ramu, S. Chongdar, K. Sarkar, A. Bhaumik, Material Today Chem., 2022, 24, 100882.
2. SMART and SAINT software package, Siemens Analytical X-ray Instruments Inc., Madison, WI, 1996.
3. (a) O.V. Dolomanov, L.J. Bourhis, R.J. Gildea, J. A. K. Howard and H. Puschmann, J. Appl. Cryst. 2009, 42, 339; (b) G. M. Sheldrick, Acta Cryst. A, 2008, 64, 112; (c) G. M. Sheldrick, Acta Cryst. C, 2015, 71, 3.
4. V. Guillerm, Ł. J. Weseliński, Y. Belmabkhout, A. J. Cairns, V. D'Elia, Ł. Wojtas, K. Adil and M. Eddaoudi, *Nature Chem*. 2014, **6**, 673.
5. A. C. Kathalikkattil, D. W. Kim, J. Tharun, H. G. Soek, R. Roshan and D. W. Park, *Green Chem*. 2014, **16**, 1607.
6. Y. W. Ren, Y. C. Shi, J. X. Chen, S. R. Yang, C. R. Qi and H. F. Jiang, *RSC Adv.* 2013, **3**, 2167.
7. P. Patel, B. Parmar, R. I. Kureshy, N. H. Khan, E. Suresh, Dalton Trans., 2018, 47, 8041-8051.
8. T. Zhang, H. Chen, H. Lv, Q. Li, X. Zhang, RSC Adv., 2021, 11, 9731.
9. S. Senthilkumar, M. S. Maru, R. S. Somani, H. C. Bajaj and S. Neogi, Dalton Trans., 2018, 47, 418.
10. Z. Zhou, C. He, J. Xiu, L. Yang and C. Duan, J. Am. Chem. Soc. 2015, 137, 15066.